

# INITIAL CHARACTERIZATION OF THE USNO CESIUM FOUNTAIN

Eric A. Burt, Christopher R. Ekstrom and Thomas B. Swanson

U. S. Naval Observatory  
3450 Massachusetts Ave. NW  
Washington, D. C. 20392 U.S.A.

## ABSTRACT

We have performed an initial characterization of the stability of the U.S. Naval Observatory (USNO) cesium fountain atomic clock. This device has a short-term fractional frequency stability of  $1.5 \times 10^{-13} \text{ }^{-1/2}$ . This short-term performance enables us to measure hydrogen maser behavior over the short to medium term. When measured against a maser co-located in the same lab with the fountain, we observe a flicker floor of  $1.5 \times 10^{-15}$  that is statistically consistent with that maser's performance. Measurements of our detection noise give an upper bound on Dick-effect noise of  $1.4 \times 10^{-13} \text{ }^{-1/2}$ . Improvements in our laser servo systems have resulted in continuous data sets from this fountain of up to 7 days.

## 1. INTRODUCTION

Working atomic fountain clocks have now become ubiquitous in the high-performance frequency standard community [1]. This success is generally due to both the excellent stability and accuracy that this device can achieve. At USNO we have undertaken a program to integrate atomic fountain clocks into the USNO timing ensemble. The mission of the Observatory does not require that any of our standards be accurate realizations of the second, only that they be stable and run continuously.

The first USNO fountain based on cesium and described in this paper has essentially two goals. First, we would like to demonstrate a short-term stability of  $1-2 \times 10^{-13} \text{ }^{-1/2}$  and a systematic floor of  $1-3 \times 10^{-16}$ . A consequence of this stability is that it will allow us to determine what hydrogen masers are doing in the medium to long-term far more precisely than previously possible. Second, this fountain is a research device that will enable us to learn how best to optimize this technology for the specific goals of the observatory, in particular, long-term continuous operation.

In this paper we will describe an initial characterization of the stability of this first USNO fountain

## 2. EXPERIMENTAL LAYOUT

The physical layout of our fountain has been described previously [2], so we will only give a brief overview here.

We collect atoms in either a MOT or molasses and launch them in a (1,1,1) geometry. The laser light for the upward and downward directed laser beams are generated by two injection seeded tapered amplifiers. The light is then transported to the vacuum chamber with optical fibers. The light exiting these fibers (and the detection light optical fiber) have power servos closed around the fiber path to reduce amplitude noise at the atoms.

The atoms are launched in two phases, the first optimized for violent acceleration and the second for final

cooling. Immediately after launch, the atoms are pumped into the  $F=4$  hyperfine levels with a repumping beam tuned to the  $F=3 \rightarrow F=4$  transition. The atoms are state-selected at the detection zone by exposure to 9.2 GHz microwaves (tuned to the  $F=4, m_f=0 \rightarrow F=3, m_f=0$  transition) from an axial loop antenna inside the vacuum chamber and a subsequent transit of a light sheet that removes remaining  $F=4$  atoms.

The microwave cavity and the drift region are enclosed in a high-performance magnetic shield set providing an axial shielding effectiveness of better than 35,000 [3]. An axial solenoid provides a 225 nT magnetic field for the cavity and free precession regions.

The entire outer shield and the part of the vacuum chamber that it encloses is held at  $44.5 \pm 0.1^\circ\text{C}$ . As a result, everything inside the shields, including the microwave cavity, the drift region and the C-field solenoid is temperature-stabilized and gradients are minimized. Making the entire outer shield an isotherm instead of temperature-stabilizing individual components contained therein greatly reduces the sensitivity of this fountain to ambient temperature fluctuations and enhances its robustness for continuous operation. The small fields generated by the resistive heaters are kept far away from the sensitive drift region. Tests indicate no detectable perturbation to the atoms due to these fields.

After making two transits of the microwave cavity the atoms return to the detection region. Both  $F=3$  and  $F=4$  atoms are detected, allowing us to calculate a signal normalized to the total atom number. We run the fountain with a typical cycle time of 1.35 seconds.

Since our last report on this fountain we have made significant changes to enhance its performance. We have optimized the phase-locked loop (PLL) between the hydrogen maser and the quartz crystal in the microwave frequency chain, located and plugged several microwave leaks, improved the detection quantization axis to stabilize the detection process, and closed several servo loops, including the repump laser intensity and the temperature servo on the outer magnetic shield.

In addition, we have made changes in the way we perform frequency modulation of our interrogation microwaves. Previously we used square-wave modulation of the interrogation frequency. Our Ramsey fringes are about 1 Hz wide so the frequency modulation used was  $\pm 0.5$  Hz. This was accomplished by frequency-modulating a digital synthesizer whose output is mixed in with the frequency chain to produce the final interrogation frequency. We found that if we instead modulate the phase of this synthesizer, leaving its frequency constant, we improve the fountain's stability. The phase is changed by  $\pm 90^\circ$  between the two microwave pulses that are part of each interrogation cycle. This approach is insensitive to fluctuations in launch height and is very similar to a scheme being considered for space-borne cold atom clocks to reduce their sensitivity to vibrations [5].

Another important change is an improvement to our laser frequency locks. Our diode lasers are locked to a saturation cell in the conventional way using an analog integrator to control the diode PZT voltage. We found that this method was stable for up to a day, but not longer. To address this deficiency we have added a digital integrator that periodically polls the laser for its PZT voltage and compares this to the servo control voltage. If the difference is outside a threshold, the digital integrator adjusts the bias PZT voltage bringing the control voltage back towards zero. This essentially gives the loop infinite gain at DC and keeps our lasers in lock for months at a time.

Finally we devised a new microwave frequency chain that has resulted in a 25% improvement in short-term stability. At the heart of the new chain, which is displayed in Figure 1, is a small commercial component containing a Step Recovery Diode (SRD) and a Dielectric Resonant Oscillator (DRO).

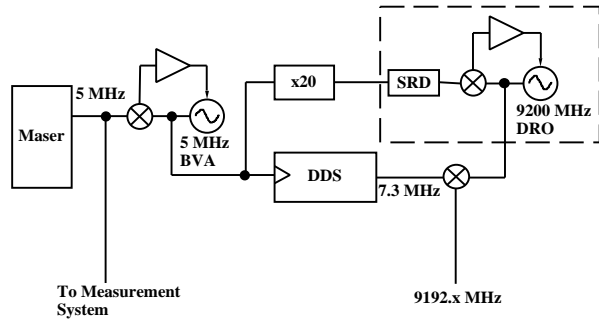


Fig. 1. The new microwave frequency chain. The dashed section is a DRO-based unit that provides the phase-coherent multiplication from 100 MHz to 9.2 GHz.

The 9.2 GHz of the DRO is phase-locked to the 92<sup>nd</sup> harmonic of the 100 MHz reference input. This output is mixed with the output of the previously mentioned digital synthesizer to produce the required interrogation frequency. The various sidebands are not suppressed, but the 300 kHz linewidth of our high-Q cavity rejects these with extreme efficiency. This chain is simple, robust and built entirely from commercially available components. In addition, the new topology allows us to insert the digital synthesizer at the top of the chain (instead of at approximately 500 MHz, as was done previously) removing a multiplicative factor of its contributed noise. While we have not fully characterized this chain yet, it has improved the short-term stability of our fountain and reduced the upper bound on our Dick-effect [4] noise.

### 3. RESULTS

Figure 2 shows the Allan deviation of frequency differences between the fountain and hydrogen maser N17, over a 7-day period. There are four features to note in this graph. First, the short-term stability is  $1.7 \times 10^{-13} \tau^{-1/2}$ . Further optimizations in the operation of our frequency chain have brought this number consistently down to  $1.5 \times 10^{-13} \tau^{-1/2}$ , as will be shown later. Second, there is a small but statistically significant deviation from white FM noise at about 5 seconds. Third, there is another deviation that begins at just under 1000 seconds. And fourth, the data appear to have a floor at around  $1.5 \times 10^{-15}$ .

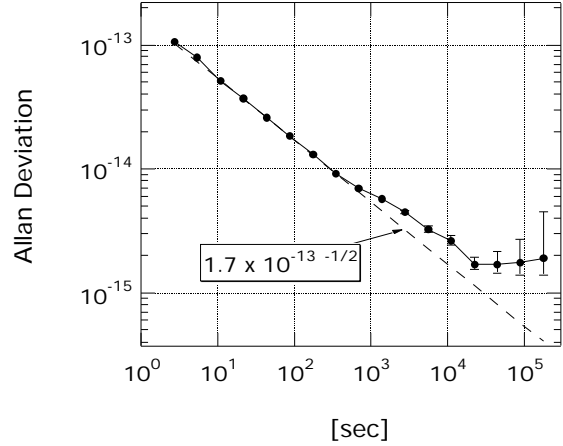


Fig. 2. Allan deviation of frequency differences between the fountain and hydrogen maser N17.

To get a better understanding of the deviations from white noise we measured the behavior of the underlying detection process. The microwave power is adjusted to give a total  $\pi/2$  pulse after two transits of the microwave cavity (instead of the usual  $\pi$ ), resulting in an even superposition of  $F=3$  and  $F=4$  states when the microwaves are on resonance. This produces a signal that is maximally frequency-insensitive [6] and does not include Dick-effect noise [4] and is therefore a good measure of detection noise. These  $\pi/4$  data are shown in Figure 3, where a short-term stability of  $6 \times 10^{-14} \tau^{-1/2}$  with no indicated floor into the mid- $10^{-16}$ s is observed.

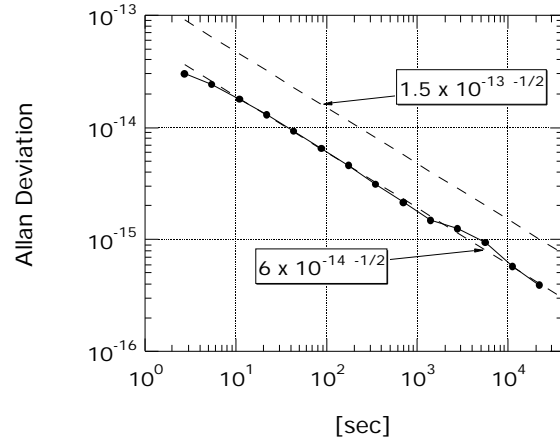


Fig. 3. Allan deviation for frequency-insensitive  $\pi/4$  data taken on resonance. The result is largely detection noise, which is shown to be much smaller than, and therefore not contributing significantly to, the total fountain noise.

This demonstrates that the detection noise does not contribute appreciably to the overall noise of the device over the indicated time scale. By comparing this to our current total short-term stability of  $1.5 \times 10^{-13} \tau^{-1/2}$  we get an upper bound on Dick-effect noise of  $1.1\text{--}1.4 \times 10^{-13} \tau^{-1/2}$ . This compares to an upper bound

of  $1.7\text{--}1.9 \times 10^{-13} \text{ }^{-1/2}$  for our previous frequency chain and agrees well with the level of Dick-effect noise that can be predicted from the phase noise of our quartz crystal.

Next, we suspected that the non-statistical characteristic at 1000 seconds in Figure 2 is due to the well-known behavior of cavity-tuned masers which exhibit a similar deviation from white noise in their Allan deviation at about this averaging time. To test this we turned the cavity tuner off for N17. We expected that this would dramatically increase the drift rate, but that the deviation from white noise at 1000 seconds would disappear. The results are shown in Figure 4.

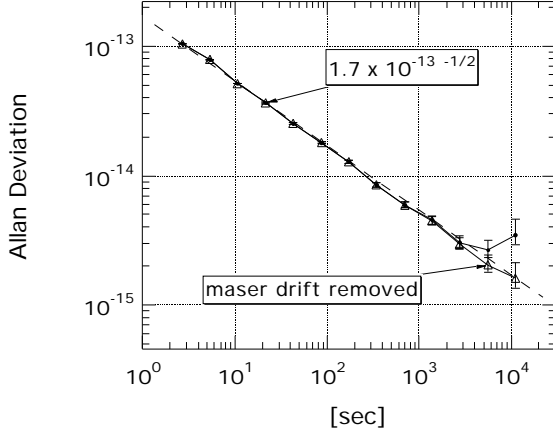


Fig. 4. Allan deviation for frequency differences between the fountain and N17 with N17's cavity tuner off. The non-statistical deviation is gone at the expense of a much larger drift as expected. The closed circles show the raw data and the open triangles show that data with the drift removed.

Indeed, the noise is completely white until it becomes dominated by the drift now estimated at about  $2 \times 10^{-14}/\text{day}$  (with the cavity tuner on, the drift for this maser is about  $4 \times 10^{-16}/\text{day}$ ). When this drift is removed, the fountain minus N17 Allan deviation is consistent with white noise.

To further verify that the 1000-second deviation in Figure 2 belongs to the maser and not to the fountain, we have been able to estimate N17's behavior by performing a three-cornered hat analysis between three masers, including N17 (Figure 5). The data for this analysis were collected over the same time period that frequency differences were monitored between N17 and the fountain. Note that the measurement system used for this comparison contributes white phase noise that has been measured to be  $8 \times 10^{-13}/\text{ }^{-1/2}$  and dominates the short-term noise of these solutions.

Figure 6 shows the fountain minus N17 data taken at the same time as the data for the three-cornered-hat analysis shown in Figure 5. These are the first data to incorporate all of the changes indicated in the previous section. The short-term stability is now  $1.5 \times 10^{-13} \text{ }^{-1/2}$  and the deviation at 5 seconds is gone (most likely due to optimization of the maser-crystal PLL).

Superimposed on this graph we have added the N17 three-cornered hat solution with measurement system noise removed and the known short-term fountain noise contribution of  $1.5 \times 10^{-13} \text{ }^{-1/2}$  added in. The latter value is justified by the fact that the maser is known to have performance significantly below  $1.5 \times 10^{-13} \text{ }^{-1/2}$  for time periods of 1 to several hundred

seconds. Thus over this time period at least, the noise is determined by the fountain.

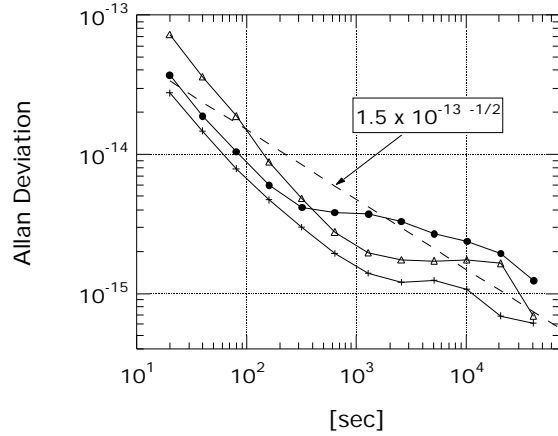


Fig. 5. A three-cornered-hat solution for masers N17 (closed circles), MC3 (open triangles) and N18 (crosses). The short term out to between 200 and 500 seconds is dominated by measurement system noise ( $8 \times 10^{-13}/\text{ }^{-1/2}$ ).

The agreement in Figure 6 between synthesized fountain minus N17 data (using the three-cornered-hat solution) and the real fountain minus N17 data is striking and supports the hypothesis that the 1000 second deviation is due to the maser's cavity tuner. In addition, the data are statistically consistent with the statement that the floor is due to N17.

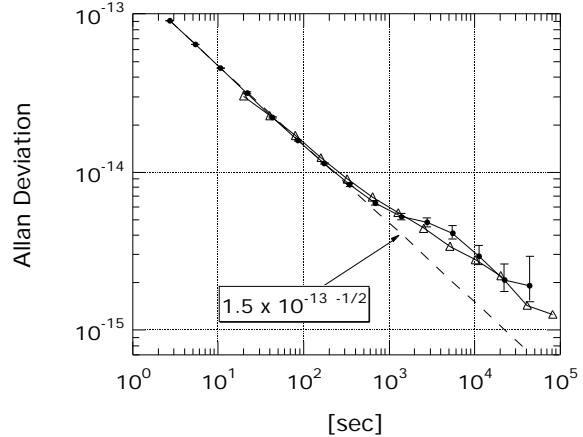


Fig. 6. Allan deviation for fountain vs. N17 (solid circles) and a synthesized estimation that assumes an entirely white FM noise contribution from the fountain (open triangles) – see text.

This type of calculation could be turned around to steer out the maser effects on paper. In the future, to gain further understanding into fountain behavior, we plan to physically steer the maser to the fountain via a synthesizer. The synthesizer would be inserted either between the maser and crystal oscillator or between the maser and the measurement system (see Figure 1). We then plan to compare the steered maser to USNO time scales. While our current data suggest that our observed noise floor may be due to the maser, proof will have to await steered operation.

#### 4. CONCLUSIONS

In conclusion, we have performed an initial stability analysis of the USNO cesium fountain. We have demonstrated a short term stability of  $1.5 \times 10^{-13} \text{ }^{-1/2}$  and have shown data demonstrating that deviations from statistical behavior at around 1000 seconds are due to the maser local oscillator's cavity tuner. In the longer term we are able to establish an upper bound for the fountain "flicker floor" of  $1.5 \times 10^{-15}$ , and have shown that these data are consistent with the hypothesis that this floor is due to the maser. We have also demonstrated continuous operation of the fountain for 7 days and see no limitations to running the maser/fountain combination in steered mode for one month or more. Thus we have reached the short- and medium-term stability goals for this device, as well as the goal of being able to measure short- to medium-term maser performance and continue to analyze long-term behavior. In addition, we have laid the basis for future continuously operating USNO fountains already under construction.

#### 5. REFERENCES

- [1] A. Clairon, et al., "Preliminary Accuracy Evaluation of a Cesium Fountain Frequency Standard," in Proceedings of the Fifth Symposium on Frequency Standards and Metrology, 1995, pp. 49-59; S. Bize, et al. "Interrogation Oscillator Noise Rejection in the Comparison of Atomic Fountains," pp. 9-11; S. R. Jefferts, et al., "Preliminary Accuracy Evaluation of a Cesium fountain Primary Frequency Standard at NIST," pp. 12-15; S. Weyers, et al., "First Results of PTB's Atomic Caesium Fountain," pp. 16-19; P. B. Whibberly, "Development of a Caesium Fountain Primary Frequency Standard at the NPL," pp. 24-26, all in Proceedings of the conference EFTF and IEEE FCS, 1999. T. Swanson, et al., "Preliminary Results from the USNO Cesium Fountain," in Proceedings of the 2000 IEEE/EIA International Frequency Control Symposium, p. 672. F. Levi et al., "Preliminary Accuracy Evaluation of the IEN Cesium Fountain" and G. Mileti et al., "Recent Developments on the ON/OFMET Continuous Cs Fountain Standard," both in these proceedings.
- [2] C. Ekstrom, et al., "The USNO Cesium Fountain," in Proceedings of the 14<sup>th</sup> EFTF, p. 502 (2000).
- [3] T. Swanson, et al., "Preliminary Results from the USNO Cesium Fountain," in Proceedings of the 2000 IEEE/EIA International Frequency Control Symposium, p. 672.
- [4] G. J. Dick, "Local oscillator induced instabilities in trapped ion frequency standards," in the Proceedings of the 19<sup>th</sup> PTTI Applications and Planning Meeting, p. 133 (1987).
- [5] W.M. Klipstein, et al., "Phase Modulation for Reduced Vibration Sensitivity in Laser-Cooled Clocks in Space", these proceedings.
- [6] G. Santarelli, et al., "Quantum Projection Noise in an Atomic Fountain: A High Stability Cesium Frequency Standard", Phys. Rev. Lett. **82**, 4619 (1999).